ELSEVIER

Available online at www.sciencedirect.com
SCIENCE DIRECT

Journal of Crystal Growth 253 (2003) 89–94

JOURNAL OF CRYSTAL GROWTH

www.elsevier.com/locate/jcrysgro

Structural characterization of epitaxial $Cd_{1-x}Zn_xTe$ semiconductor thin films by ion beam techniques

F. Fernández-Lima[a], E.M. Larramendi[b], E. Purón[b], E. Pedrero[b], O. de Melo[b], D.L. Baptista[c], F.C. Zawislak[c,*]

[a] *Institute of Nuclear Science and Technology of Havana, Cuba*
[b] *Physics Faculty, IMRE, University of Havana, Cuba*
[c] *Instituto de Física, Universidade Federal do Rio Grande do Sul, C.P. 15051, Porto Alegre 91501-970, Brazil*

Received 15 May 2002; accepted 20 October 2002
Communicated by M.S. Goorsky

Abstract

We report on the structural characterization of ZnTe, CdTe and $Cd_{1-x}Zn_xTe$ epilayers grown on GaAs(1 0 0) by isothermal closed space sublimation epitaxy. A detailed study of the heterostructures based on conventional Rutherford backscattering spectrometry, ion channeling and nuclear reaction analysis allows to determine the thickness, composition, impurities, lateral homogeneity and interface structure of the grown thin films. The growth rates were determined for the extreme composition (ZnTe, CdTe). Stoichiometry and lateral homogeneity were observed in ZnTe and CdTe films. Low carbon contamination homogeneously distributed in the film was present and no oxygen contamination of the samples was observed. The channeling analysis of ZnTe films allowed to evaluate the thickness of the interface damaged region.
© 2003 Elsevier Science B.V. All rights reserved.

PACS: 81.05.Dz; 81.15.Kk; 68.55.Jk; 61.85

Keywords: A1. Characterization; A3. Vapor phase epitaxy; B1. Alloys; B2. Semiconducting II–VI materials

1. Introduction

II–VI semiconductors have great interest for their optoelectronic applications. High-quality heterostructures have been obtained only using a few techniques, such as molecular beam epitaxy (MBE) [1,2], metal-organic chemical vapor deposition (MOCDV) [3–5] and ultrahigh vacuum atomic layer epitaxy (UHV–ALE) [6,7]. Some of these techniques use toxic products, all are very expensive and technologically sophisticated. However, recently II–VI semiconductor epitaxial films were obtained using a simple and cheap isothermal close space sublimation and epitaxy (ICSSE) technique [8,9]. In the present paper, CdTe and ZnTe samples grown by the ICSSE technique are characterized by ion beam analysis methods such as Rutherford backscattering spectrometry (RBS),

*Corresponding author. Tel.: +55-51-331-66427; fax: +55-51-331-66510.
E-mail address: zawislak@if.ufrgs.br (F.C. Zawislak).

0022-0248/03/$ - see front matter © 2003 Elsevier Science B.V. All rights reserved.
doi:10.1016/S0022-0248(03)01023-6

channeling and nuclear reaction analysis (NRA), to study the thickness, composition, impurities, lateral homogeneity, and interface structure. These parameters are very important in order to evaluate the quality and usefulness of the films grown by ICSSE.

2. Experimental details

Samples were grown using an isothermal closed space sublimation and epitaxy technique. The characteristics of this technique have been reported elsewhere [8,9]. A GaAs substrate was exposed to Zn, Cd and Te elemental sources alternately in each case. A specially designed graphite crucible keeps a constant temperature of the whole close space configuration system. Under these conditions, the only driving force for the film growth is vapor pressure difference between the elemental source and the previously grown film surface. Once the growing surface is fully covered with the atoms of the elemental source, the vapor pressure difference disappears due to the equilibrium between the growing surface and the pure element vapor. Then the substrate is shifted to the other source, concluding a cycle once equilibrium is reached at this second stage. Using this procedure an atomic layer epitaxy regime is obtained for ZnTe with a growth rate of 1 monolayer per cycle. When the substrate is transferred, from one source to other, the residual gas remaining in the substrate compartment is purged in H_2 atmosphere. The exposition times of the substrate to each elemental source τ_s, and at the purge hole τ_h are shown in Table 1. The ternary alloy was obtained, following the sequential period Te–Zn–Te–Cd and so on until 60 cycles. GaAs (1 0 0) oriented substrates were previously cleaned using typical H_2SO_4:H_2O_2:H_2O (5:1:1) etching. The growth temperature was set at 385°C and the process occurs in Pd purified H_2 flux at atmospheric pressure.

The ion beam analyses were made using the 3 MV TANDETRON accelerator of the Instituto de Física, Universidade Federal do Rio Grande do Sul, Brazil. The RBS analysis of the samples was performed with ^{4}He ions of 1.0 MeV. A surface barrier detector with 12 keV FWHM at an angle of 165° was used. The RBS spectra were processed with the program RUMP [10]. The carbon and oxygen profiles were determined by NRA. A strong resonance of the ^{12}C(α,α) ^{12}C reaction at 4.265 MeV [11] and ^{16}O(α,α) ^{16}O reaction at 3.045 MeV [12] were used in the same experimental setup. For channeling experiments, samples were analyzed in the same setup introducing a goniometer with a computer interface in the chamber. Measurements were made using a 0.2° step running.

Transmission electron microscopy (TEM) observation was performed using a JEM 2010 200 kV microscope of the Physics Department, CINVESTAV, Mexico, DF.

3. Results and discussion

The growth regime, areal density, growth speed and stoichiometry of the obtained thin films were

Table 1
Growth regime, exposition time of the substrate to each elemental source τ_s and at the purge hole τ_h, areal densities, thickness and growth rate of the samples

Sample	Stoichiometry	τ_s (s)	τ_h (s)	Cycles	Areal density (1015 cm^{-2})	Thickness (nm)	Growth rate (nm/cycle)
C34	ZnTe	3	3	375	365±5	103.6±1.4	0.27±0.01
C2	ZnTe	3	3	80	75±5	21.3±1.4	0.27±0.02
C22	ZnTe	3	3	375	375±10	106.3±2.8	0.28±0.01
C18	CdTe	8	3	120	380±5	124.5±1.6	1.03±0.01
C43	CdTe	10	10	200	755±5	247.4±1.6	1.24±0.01
C35	$Cd_{0.55}Zn_{0.45}Te$	3	0	60[a]	100±5	30.6±1.5	0.31±0.01

[a] Cycles of the Te–Zn–Te–Cd sequential period.

determined from the analysis of the RBS spectra. The results are shown in Table 1. Thickness was obtained from the areal density using the bulk density of ZnTe and CdTe, respectively. The density of the alloys was calculated considering a linear dependence of density with composition. In all cases was considered a crystallographic density (as calculated from the reported lattice parameters) due to the crystalline quality of the samples (0.035245 atom $\times$ Å^{-3} for ZnTe and 0.030517 atom $\times$ Å^{-3} for CdTe). The growth rate (in nm/cycle) was calculated using the thickness of the obtained samples. In the case of ZnTe samples the growth rate was slightly lower but close to one monolayer per cycle regimen (one monolayer $\sim$0.3 nm for ZnTe). In the case of CdTe samples the growth speed was larger than 1 nm/cycle. The differences can be ascribed to Cd transport from one source to the other during the growth process, because Cd has a very large vapor pressure as compared to Zn or Te [9]. The dependence of the thickness with the number of cycles for both ZnTe and CdTe is shown in Table 1. These growth rate results are in agreement with those calculated from reflectivity measurement and TEM [8,9].

In all cases ZnTe and CdTe showed a 1:1 stoichiometry as expected for binary compounds without metal inclusions. For the $Cd_{1-x}Zn_xTe$ alloy, the value of $x = 0.45$ was determined from the RBS analysis. Attending to the growth rates obtained for ZnTe and CdTe, values of $x \sim 0.2$ and growth rate $\sim$0.7 nm/cycle would be expected for the ternary alloy. However, the results show more incorporation of Zn and less of Cd. Recently, we have obtained this behavior in similar samples [9]. It is explained assuming that the substitution of Cd by Zn at the CdTe rich surface could take place under Zn exposure. This effect could produce large incorporation of Zn because Cd from the inner layers can diffuse to the surface and be substituted there by Zn as well.

In order to study lateral homogeneity of the films, two samples C34 (pure ZnTe) and C35 ($Cd_{0.55}Zn_{0.45}Te$) have been analyzed using RBS at different positions from the center to the border (the diameter of the films is around 9 mm). The obtained spectra at various positions are shown in Figs. 1(a) and (b). The spectra show that for both

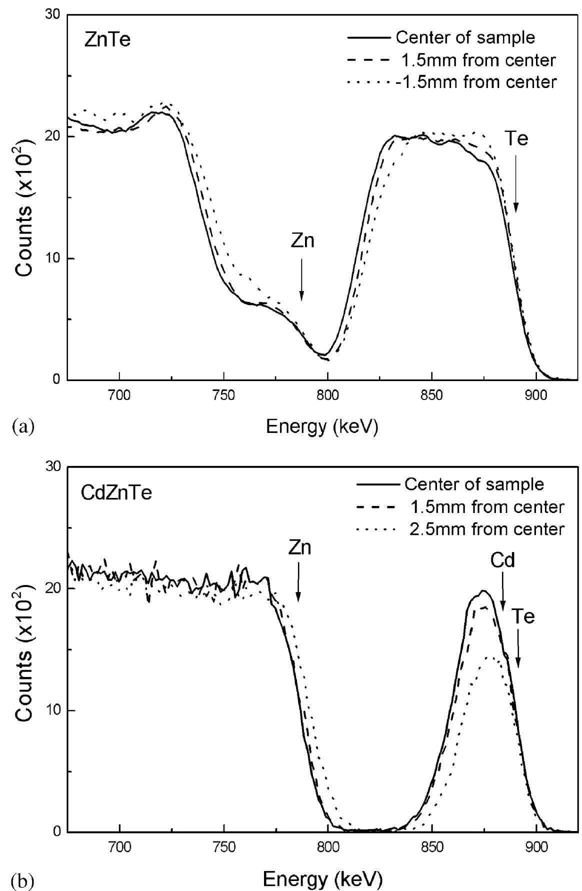

Fig. 1. 1.0 MeV $^4He^+$ beam RBS spectra of samples: (a) C34 (pure ZnTe) and (b) C35 ($Cd_{0.55}Zn_{0.45}Te$) measured at different positions.

samples there is a small decrease of thickness towards the border of the samples within a radius of $\pm$1.5 mm. We observe a larger thickness decrease in sample C35 at a radius of 2.5 mm from the center. Nevertheless, at all the measured positions, the RBS spectra show the correct stoichiometry and composition of the samples. The thickness non-homogeneity could be due to small temperature gradients in the substrate.

Since purity is a very important parameter for semiconductor thin films, we take advantage of ion beam analysis to determine contaminants in the samples. The carbon contamination was obtained from the analysis of the strong resonance spectrum in the $^{12}C(\alpha,\alpha)^{12}C$ reaction at 4.265 MeV. Carbon

contamination of the sample C34 was measured at two different deeps varying the beam energy. A pure carbon film pattern was used for calibration purpose. The results show that sample C34 presents a carbon contamination of 4% (molar fraction) near to the surface and decrease to 2% near the ZnTe/GaAs interface. The error in the measured carbon concentration is about 10%. X-rays diffraction analysis did not show evidences of any carbon-related phase. These results show that only a very small carbon contamination homogeneously distributed in the film is present. The contamination could come from the graphite crucible or also from impurity related with the chemical etching of the substrate. No oxygen contamination of the samples was observed as shown by the analysis via the resonance of the $^{16}O(\alpha,\alpha)$ ^{16}O reaction at 3.045 MeV. This result was expected taking into account the quality of the Pd purified hydrogen.

The defects present at the ZnTe/GaAs interface can be seen in the TEM micrograph of Fig. 2, for a ZnTe film of 30 nm. However a better quantitative description of the defect distribution as function of the film thickness is obtained from the channeling data. The channeled and random spectra of sample C34 are displayed in Fig. 3. The aligned spectrum shows a fairly strong increase in the dechanneled fraction with increasing the beam penetration depth into the ZnTe layer, indicating that the defects are localized in the region close to the ZnTe/GaAs interface. Fig. 3 shows that the RBS Te signal spectrum is well separated from Zn as well as from the Ga and As ones, allowing us to analyze the sample dechanneled fraction without spurious effects due to RBS signal overlapping.

Thus, useful information can be obtained on the distribution and evolution of the defects occurring into the ZnTe epilayers by comparing the epilayer normalized channeling yield X_d (i.e. the channeled aligned RBS normalized to the random yield) to the corresponding yield X_v of a perfect crystal. To this purpose, the dechanneling probability [13] can be defined as

$$P_d(x) = \ln\left(\frac{1 - X_v(x)}{1 - X_d(x)}\right),$$

where x is the distance from the ZnTe surface. We assume $X_v(x)$ values equal to the semi-empirical estimated value of 4.1% for an ideal ZnTe crystal [14]. In Fig. 4, the values of $P_d(h - x)$, where h is the film thickness, are shown as a function of the distance from the ZnTe/GaAs interface. Two different regions can be distinguished in the $P_d(h - x)$ profile: the first region, where a sharp

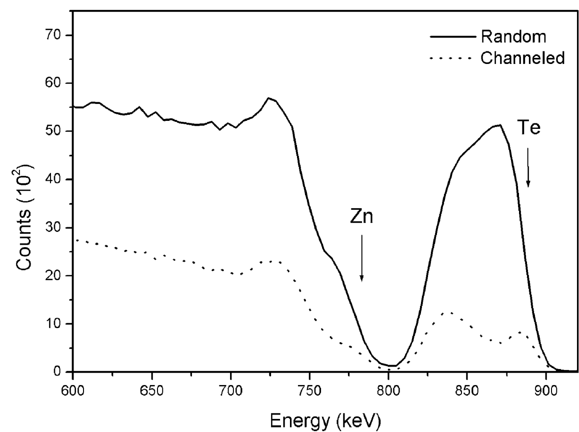

Fig. 3. 1.0 MeV $^4He^+$ beam RBS channeled and random spectra of sample C34 (pure ZnTe).

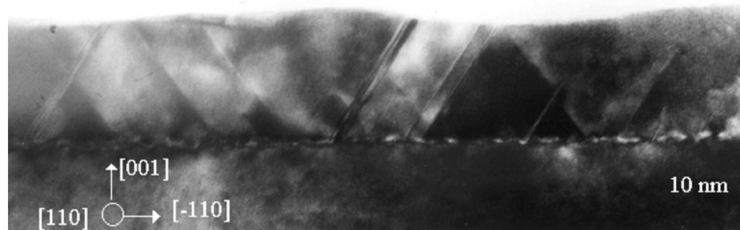

Fig. 2. Transmission electron micrograph (cross-section) for a ZnTe sample of 30 nm.

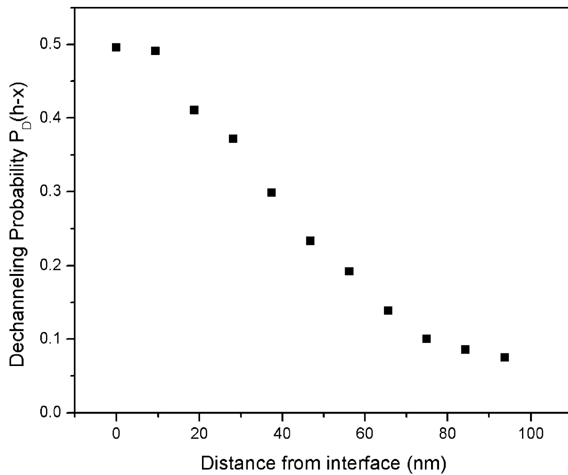

Fig. 4. Dechanneling probability as function of the distance from the ZnTe/GaAs interface.

decrease of the dechanneled fraction with increasing the distance from the interface is observed, whereas a much lower decrease of $P_d(x)$ is observed in the second region starting about 60–70 nm from the interface. As the dechanneled fraction is proportional to the local defect concentration in the layer, the above results reveal that most of the defects occurring in the ZnTe film are located in the 70 nm-thick region close to the interface, and that outside this region there is a smaller, practically constant, defect concentration. This effect is probably caused by the influence of the ZnTe/GaAs interface since this heterostructure presents a lattice mismatch of around 7%. This lattice mismatch is accommodated in a dislocation misfit array that probably generates several other defects (stacking faults for example). The analysis of the channeling experiment reveals clearly that the damaged region extended for almost 70% of the C34 film with thickness of ~100 nm. Beyond this 70 nm-thick region, the dechanneled fraction indicates that further defects do not occur in the epilayer, showing that there is practically no substrate influence beyond this first region. The same behavior has been also observed in ZnTe/GaAs heterostructure grown by more expensive and sophisticated growing techniques such as metalorganic vapor phase epitaxy (MOVPE) [15] and MBE [16].

4. Conclusions

ZnTe, CdTe and their ternary alloy grown by ICSSE were characterized using ion beam analysis techniques. The growth rates were determined for different samples: an atomic layer epitaxy regime was observed for ZnTe while larger than one monolayer/cycle rates were obtained for CdTe samples. This agrees with previous results [8,9] and is considered to be due to Cd transport from one source to the other during the movement of the substrate. Both binary compounds show good lateral homogeneity and the expected metal/tellurium 1:1 stoichiometry. The lateral homogeneity was poorer in $Cd_{1-x}Zn_xTe$ alloys with a decreasing thickness towards the border of the film. A low carbon contamination homogeneously distributed in the film was present; it could come from the graphite crucible or from any impurity related with the chemical etching of the substrate. No oxygen contamination of the samples was observed. The channeling experiment reveals that the more damaged region extends for 70 nm from the interface of ZnTe/GaAs heterostructure grown by ICSSE. Beyond this region, the dechanneling rate indicates a much lower defect concentration in the epilayer, indicating that there is no substrate influence beyond this region.

Acknowledgements

The support of the Brazilian Agencies FINEP/PRONEX and CNPq and the Alma Mater project from the University of Havana are acknowledged. One of the authors (F. Fernández-Lima) thanks the Centro Latino Americano de Física (CLAF) for financial support. The authors are indebted with Dr. M. Tamura for TEM micrograph.

References

[1] V.I. Kozlovsky, A.B. Krysa, Yu.V. Korostelin, Yu.G. Sadofyev, J. Crystal Growth 214–215 (2000) 35.
[2] R.H. Miles, G.Y. Wu, M.B. Johnson, T.C. McGill, J.P. Faurie, S. Sivananthan, Appl. Phys. Lett. 48 (1986) 1383.
[3] E.J. Mayer, N.T. Pelekanos, J. Kuhl, N. Magnea, H. Mariette, Phys. Rev. B 51 (1995) 17263.

[4] M. Levy, N. Amir, E. Khanin, A. Muranevich, Y. Nemirovky, R. Beserman, J. Crystal Growth 187 (1988) 367.
[5] K. Cohen, S. Stolyarova, N. Amir, A. Chack, R. Beserman, R. Weil, Y. Nemirovky, J. Crystal Growth 198/199 (Part 2) (1999) 1174.
[6] J.T. Sadowski, M.A. Herman, Appl. Surf. Sci. 112 (1997) 148.
[7] J.T. Sadowski, M.A. Herman, Thin Solid Films 306 (1997) 266.
[8] E.M. Larramendi, E. Purón, L.C. Hernández, M. Sánchez, S. De Roux, O. de Melo, G. Romero-Paredes, R. Peña-Sierra, M. Tamura, J. Crystal Growth 223 (2001) 447.
[9] S. Tobeñas, E.M. Larramendi, E. Purón, O. de Melo, F. Cruz- Gandarilla, M. Hesiquio-Garduño, M. Tamura, J. Crystal Growth 234 (2002) 311.
[10] L.R. Doolittle, Nucl. Instrum. Methods Phys. Res. B 9 (1985) 344.
[11] Y. Feng, Z. Zhou, Y. Zhou, G. Zhao, Nucl. Instrum. Methods Phys. Res. B 86 (1994) 225.
[12] Li Jian, L.J. Matienzo, P. Revesz, Gy. Vizkelethy, S.Q. Wang, J.J. Kaufman, J.W. Mayer, Nucl. Instrum. Methods Phys. Res. B 46 (1990) 287.
[13] L.C. Feldman, J.W. Mayer, S.T. Picraux, Materials Analysis by Ion Channeling, Academic, New York, 1982.
[14] N. Lovergine, R. Cingolani, G. Leo, A.M. Mancini, L. Vasanelli, F. Romanato, A.V. Drigo, M. Mazzer, Appl. Phys. Lett. 63 (1993) 3452.
[15] G. Leo, M. Longo, N. Lovergine, A.M. Mancini, L. Vasanelli, A.V. Drigo, F. Romanato, T. Peluso, L. Tapfer, J. Vac. Sci. Technol. B 14 (1996) 1739.
[16] N. Lovergine, L. Liaci, J-D. Ganière, G. Leo, A.V. Drigo, F. Romanato, A.M. Mancini, L. Vasanelli, J. Appl. Phys. 78 (1995) 229.